

# Reduction of Porosities in Pulse-MAG Welding of Galvanized Steel Sheets for a Zero-Gap Lap Joint Configuration



Yuqian Huang, Wangteng Lin, Xiao Wei, Shaofeng Yang,  
Wei Huang, Wang Zhang, Jijin Xu, Junmei Chen, Chun Yu  
and Hao Lu

**Abstract** Pulse-MAG welding was conducted to joint lap fillet welds of galvanized steel sheets with zero-gap. During the welding process, metal transfer and molten pool were observed. A stable opening in the molten pool could become an escape path for zinc vapor. High current and welding travel speed could expand the opening. To obtain a stable opening, arc voltage needs to be controlled in a reasonable range. Besides, the exorbitant voltage and travel speed caused BCM humps and GRM humps respectively. With high current, moderate voltage and suitable travel speed, the stable opening of molten pool was created to promote the degassing of zinc vapor so that the amount and size of porosity in the weld beam were reduced.

**Keywords** Porosity · Pulse-MAG · Intelligence manufacturing  
Molten pool · Metal transfer · Opening

## 1 Introduction

Recently, the automotive industry is increasingly using galvanized steel sheets to improve long-term quality and to adapt thinner sheets for weight reduction. However, galvanized steel sheets are very poor in weldability compared with ordinary steel sheets. The boiling point of zinc is 906 °C, while during welding the temperature at which steels begin to melt is above 1300 °C [1]. Consequently,

---

Y. Huang · W. Lin · X. Wei · S. Yang · J. Xu · J. Chen · C. Yu (✉) · H. Lu (✉)  
Key Lab of Shanghai Laser Manufacturing and Materials Modification,  
School of Materials Science and Engineering, Shanghai Jiao Tong University,  
Shanghai 200240, China  
e-mail: yuchun1980@sjtu.edu.cn

H. Lu  
e-mail: shweld@sjtu.edu.cn

W. Huang · W. Zhang  
Air Liquide (China) Research & Development Co. Ltd, Shanghai 201111, China

during welding, zinc is vaporized, and zinc vapor is caught in the molten pool together with air. When zinc vapor fails to escape from the molten pool before the molten pool solidifies completely, the porosities like blowholes and pits form in the weld beam [1–4]. Furthermore, when welding is performed at high speed, this zinc vapor causes a big challenge to successfully obtain sound lap joints. Meanwhile, zinc vapor blows off welding droplets and molten pools, which increases the amount of spatter.

The defects especially the pits probably decrease the strength and fatigue property of lap joints due to the decrease of effective cross-sectional area of weld beam. Therefore, the porosity of galvanized steel sheets is always a key research object.

Previous researchers have proposed some theories and methods to inhibit the defects in different aspects. Removing the zinc layer mechanically is an extremely effective method [5]. Setting a gap between the sheets before welding was suggested by the American welding society in GMAW fillet welding [6]. Pennington [7] patented a method of laser welding of galvanized steel by replacing the zinc layer with the nickel layer. Mazumder et al. [8, 9] presented a technique that sandwich a thin copper sheet between two galvanized steel sheets. Before the steel is melted, the copper can be alloyed with the zinc. However, setting a gap or replacing the zinc layer would slower the manufacture and increase the cost. Hence, the researchers were attracted to finding a method to suppress the porosities without additional step in the process. Gualini et al. [10, 11] used dual laser beam to weld the galvanized steel sheets in a zero-gap lap joint configuration. A slot was cut by the first laser beam, and then the joint was welded by the second beam. Gu et al. [12] enlarged the molten pool of laser welding with another arc torch to provide more space for the escape of zinc vapor. With these methods, it was still possible that porosities and spatters appeared in the weld beam. And the appliance was limited owing to the cost and the welding accessibility.

The optimization of process was another practical approach to improve the welding quality of galvanized steel sheets. Matsui et al. [13] analyzed the origin of porosity and stated that the main cause of porosity was the vapor generated from the zinc layer between two sheets. The method of oxidizing zinc by increasing the oxygen content of shield gas was used to suppress the porosity. Schmidt et al. [14] investigated the keyhole oscillations during the YAG laser lap-welding of galvanized steel sheets and attempted to stabilize the keyhole movement to degas the zinc vapor. Ahsan et al. [15] investigated the porosity formation mechanisms in CMT mode. They found that in high heat input region and low heat input region, the porosity was not significant; in the middle heat input region, the porosity achieved the maximum. These researches contributed to the understand of porosity formation. But the improvement of weld beam was not significant. Izutani et al. [16] observed the formation of porosity through a high-intensity X-ray radiography imaging system. In pulse-MAG welding, the origin points of porosity formed under the arc directly. Degassing the zinc vapor directly instead of mixing in the molten pool would be a promising approach for reducing porosities. Kodama et al. [17] performed MAG welding and observed the opening of molten pool under the arc.

The density of blowholes changed with different openings. That means it could be a path for zinc vapor to escape. Therefore, the influence factors need to be studied to create an appropriate opening to degas the zinc vapor.

In this study, the different currents, arc voltages and travel speeds were employed to weld galvanized steel sheets and their influences on the opening were analyzed. To broaden the applied range, the pulse-MAG welding of galvanized steel sheets was investigated with mainstream equipment and materials in automotive field.

## 2 Experimental

The galvanized steel sheets were 1.4 mm thickness and double sides galvanized with about 12  $\mu\text{m}$  thickness zinc layer. The length of the sheet sample was 300 mm, and the width was 60 mm. In tests, the geometry with 40 mm overlap was selected, and a force was applied upon the upper sheet by the clamp to guarantee the zero gap. The surfaces of sheets were cleaned with alcohol before welding. Besides, ER50-6 solid filler wire of 1.2 mm in diameter was set to feed at a feed speed of 7.3 m/min.

The welding was implemented by a FUNAC M-20iA robot and a Fronius TransPuls Synergic 5000 power source. The gesture of welding gun was modified by the robot. The torch angle was  $60^\circ$  throughout this study. When welding the torch was fixed and the mobile platform led the sheets to move with respect to the torch. For observation of molten pool, the high-speed camera was used at 4000 frames per second. Besides, the signals of current and voltage were measured by a voltage and current measure system. The experimental set-up is shown in Fig. 1a.

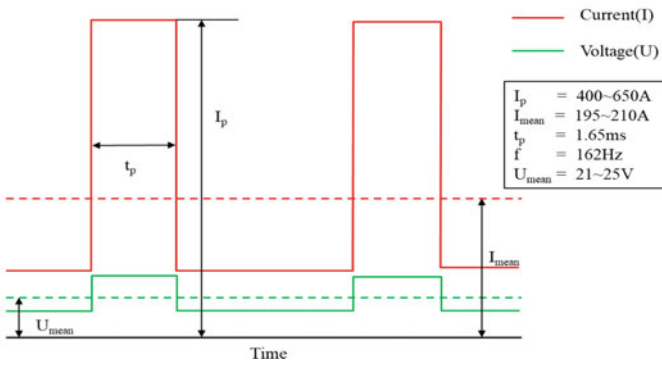
In this study, the influences of current, arc voltage and travel speed on appearance and porosity of the weld beam were investigated. The relevant parameters of welding are presented in Fig. 1b. The total heat input is the integration of the products of currents and voltages. In addition, 92% Ar + 8% CO<sub>2</sub> was used as shield gas and the flow rate was 20 L/min. The welding was performed at 1.0, 1.35 and 1.6 m/min in welding speed.

## 3 Results and Discussion

In the experiments, the upper edge of upper sheet and the surface of lower sheet were closer to the tip of wire compared with the lower edge of upper sheet, so the upper edge and the upper surface obtained higher heat input accordingly and melted more. Consequently, the butterfly-shape molten pool was formed, and the opening was observed (as shown in Fig. 2). This opening would act as a path for escaping of zinc vapor.

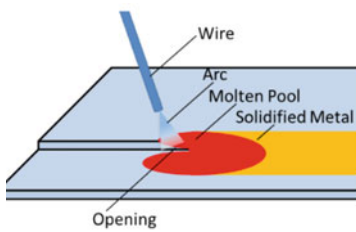


(a) Experimental set-up for welding and observation

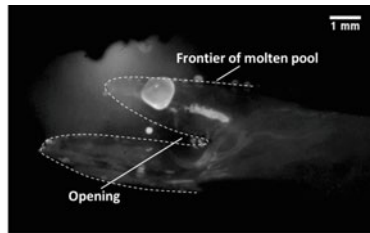


(b) Schematic diagram of pulse waveform

Fig. 1 Experimental set-up and welding parameters



(a) Schematic diagram of molten pool



(b) Molten pool observed

Fig. 2 Butterfly-shape molten pool

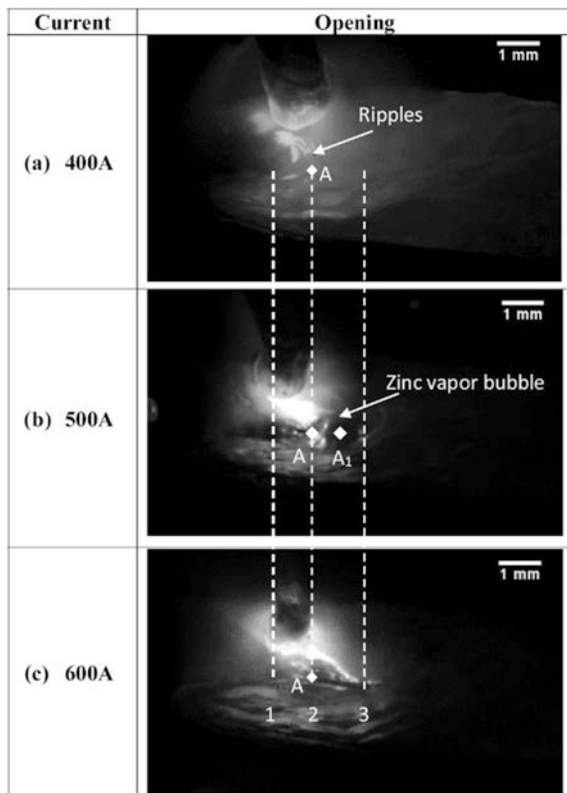
### 3.1 The Influence of Current

To investigate the influence of current in pulse-MAG welding of galvanized steel sheets. The peak currents of 400, 500 and 600 A were used in the tests. The opening of molten pool was observed in each test, but it existed a difference in the size (as seen in Fig. 3). In Fig. 3, line 1, line 2, and line 3 represent the end of opening corresponding to the peak current of 400, 500 and 600 A, respectively. Point A represents the position pointed by the tip of wire.

It's obvious that the opening of 400 A didn't extend to the point A (Fig. 3a). Point A is directly under the arc, and the origin point of porosity generates under the arc [13], so the porosity originates at the point A. With peak current of 400 A, the point A was covered by the liquid layer of molten pool. Therefore, zinc vapor totally mixed in the molten pool. Some zinc vapor escaped from the liquid layer, so the ripples left behind were observed.

Besides, the zinc vapor needed time  $T_e$  (s) to grow and escape after origination. During this period, the torch was still moving with respect to the sheets. Therefore, the escape point of zinc vapor is behind the point A. In the Fig. 3b, the point  $A_1$

**Fig. 3** Opening at peak current of 400, 500 and 600 A



represents the assumed position where the zinc vapor bubble escape. And the displacement  $D_e$  (mm) between A and  $A_1$  could be estimated as in Eq. 1:

$$D_e = T_e \cdot v \quad (1)$$

where  $v$  means the travel speed (mm/s). Undoubtedly,  $D_e$  is positive. In the condition of 500 A peak current, the opening just extended to the point A (Fig. 3b), so to any positive  $D_e$ , the point  $A_1$  would be covered by the liquid layer. The zinc vapor escaped at the point  $A_1$  would mixed in the molten pool and could cause the bulge of liquid layer near the gap (Fig. 3b).

The opening at 600 A peak current is significantly larger than the rest two (Fig. 3c) and the bulges or ripples caused by the zinc vapor were not observed in this condition. The actual point  $A_1$  was probably covered by the opening. And thus, more zinc vapor could escape to the air through the opening directly. In this way, the porosity could reduce substantially.

### 3.2 The Influence of Arc Voltage

In arc welding, there is a positive correlation between the arc length and the arc voltage. In the experiments, the sheets were welded in 21, 23 and 25 V respectively. There were significant differences in their droplet transfer cycles (Fig. 4). It is obvious that the higher arc voltage, the longer arc length according to the images at the 0 ms of cycles (Fig. 4a). At the 1 ms of cycles (Fig. 4b), the area influenced by the arc expanded with the increase of arc length. Therefore, the molten pool was larger due to higher arc voltage. And the arc shapes were irregular shape. For instance, the arc shape of 23 V seems like to consist of a typical bell-shaped arc and a bump in the outline. That's probably because zinc vapor escaped from below to the air and bulged the arc plasma partially. Similarly, the droplet in the condition of 21 V was possibly blown by the zinc vapor to deviate from the direction of wire and the deviation disturbed the metal transfer. During the period of detachment and transfer (Fig. 4c–f), the droplet in the condition of 21 V grew so large that stronger detaching force was required [18], and it couldn't be detached from the tip of wire. Consequently, the short-circuiting transfer happened in this condition and caused numerous spatters (Fig. 4g). In the condition of 23 or 25 V, there was an evident opening in the molten pool during the cycle and the gap between two sheets was exposed through the opening (Fig. 4c–f). Compared with 23 V, in the condition of 25 V, the opening was larger, and the droplet detached earlier. Due to higher detachment position, the droplet at 25 V possessed larger momentum when touching the molten pool, so the molten metal in the molten pool surged and covered a part of exposed gap (Fig. 4e–f).

The weld beam of 21 V presented some pits, because the zinc vapor mixed in the molten pool and couldn't escape from the molten pool completely. However, in the condition of 23 V, zinc vapor generated from the gap could escape through the

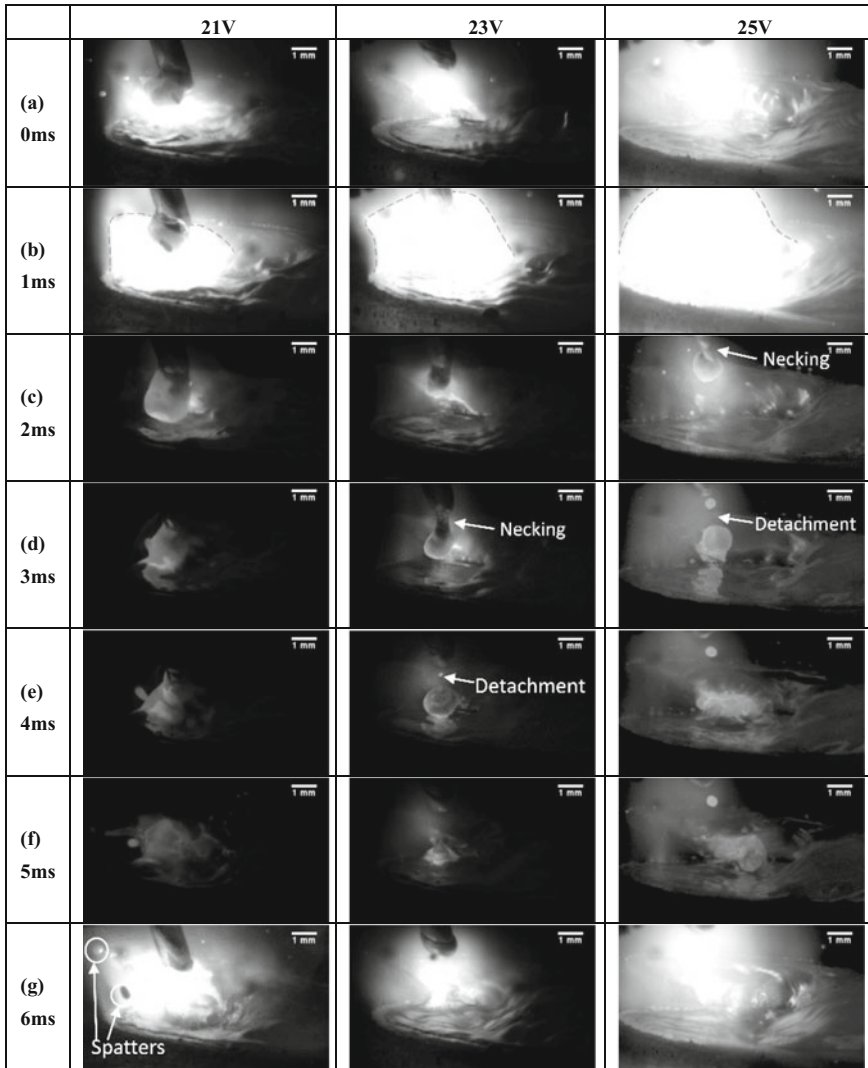


Fig. 4 Droplet transfer cycles in 21, 23 and 25 V

opening directly, so the zinc vapor mixing in the molten pool reduced massively. And thus, there were fewer pits in the weld beam of 23 V. In the condition of 25 V, the opening was not stable because of the transferred droplet and surging molten pool. The zinc vapor was impeded and thus there were some large blowholes in the weld beam. In addition, some beaded cylinder morphology (BCM) humps appeared in the weld beam of 25 V and the humps located at the upper edge of upper sheet (Fig. 6a). Hence, the voltage should be controlled in a reasonable range.

### 3.3 The Influence of Travel Speed

The travel speed influences the quality of weld beam distinctly. In this study, the influence of travel speed was investigated by the tests at 1, 1.35 and 1.6 m/min. The travel speed was modified by the mobile platform and other parameters were constant.

In arc welding, the heat input per unit  $Q$  (J/mm) can be defined as in Eq. 2:

$$Q = \frac{\eta \cdot U \cdot I}{v} \quad (2)$$

where,  $\eta$  is the arc efficiency;  $U$  is the voltage (V);  $I$  is the current (A); and  $v$  is the travel speed (mm/s). Except the melt from base metal, the transferred metal is another source of molten metal. The amount of transferred metal per unit of length can also be defined in the following formula:

$$w_t = \frac{F \cdot S \cdot \rho}{v} \quad (3)$$

where,  $F$  is the wire feed speed (mm/s);  $S$  is the cross area of wire (mm<sup>2</sup>);  $\rho$  is the density of wire (g/mm<sup>3</sup>); and  $v$  is the travel speed (mm/s). It indicates that the travel speed is in inverse proportion to the amount of transferred metal per unit of length. Therefore, the fusion metal in molten pool at higher travel speed is less due to less melt of base metal and less transferred metal. In experiments, the molten pool was in accordance with this regulation.

With the increase of travel speed, the thickness of molten metal in the molten pool decreased, but the opening of travel speed elongated. At 1 m/min, the molten metal was so much that the position pointed by the arc was covered by the molten metal completely (Fig. 5a). However, at 1.35 or 1.6 m/min, the opening was obvious (Fig. 5b–c).

Consequently, only the weld beam at 1 m/min presented some pits. At 1.35 m/min, a sound weld surface was obtained. But in the weld beam at 1.6 m/min, it appeared some gouging region morphology (GRM) humps [19], including unfilled openings and side channels (Fig. 6b). But in the humps, there was no pit or

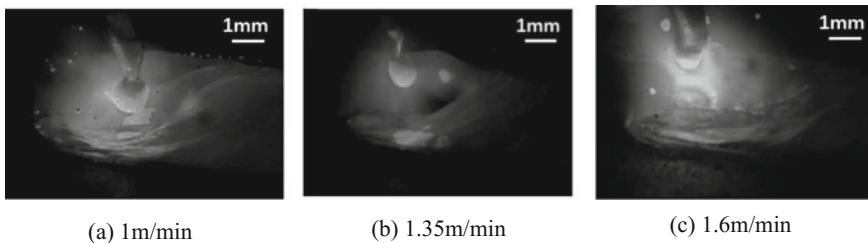


**Fig. 5** Molten pools at different travel speeds

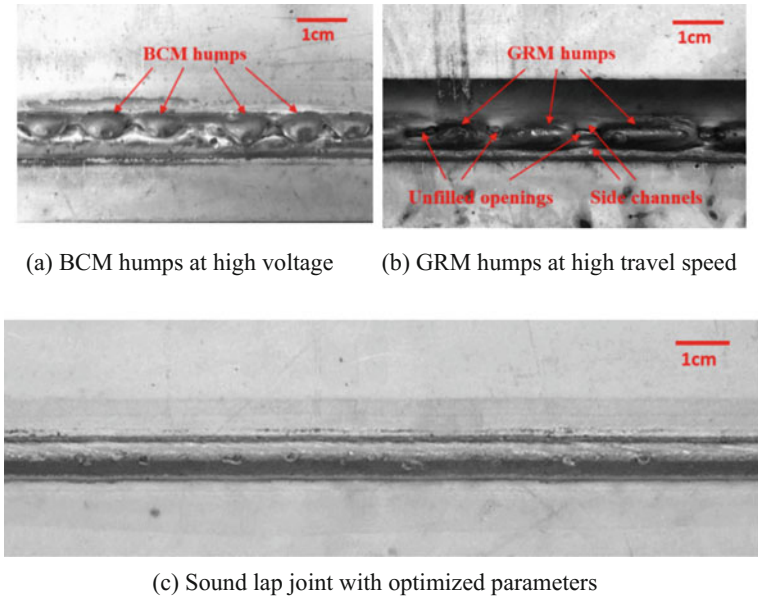


**Fig. 6** Comparison of welding surfaces in different conditions

blowhole and that probably means the zinc vapor refrained from mixing in the molten pool. The higher travel speed could reduce the porosities but cause the poor weld appearance.

### 3.4 The Analysis of Molten Pool

The opening in molten pool was observed in most experiments clearly. And this is considered to have caused the different molten pool (Fig. 7). The opening divided the molten pool into two parts: upper and lower. In molten pool, the upper forepart was relatively round while the lower forepart was board and thin (Fig. 7c). At the junction of the end of opening and the molten pool, molten metal forms a slope under the arc force (Fig. 7b). On the surfaces of the upper forepart, the lower forepart and the junction, the points under the arc were exerted by arc force ( $F_a$ ), hydrostatic force ( $F_h$ ) and surface tension ( $F_s$ ). In the horizontal direction, to keep the balance, the forces should meet the requirement as shown in Eq. 4:

$$F_a = F_h + F_s \tag{4}$$

where the directions of forces should be considered. Arc force and hydrostatic force can be calculated in following formulas:

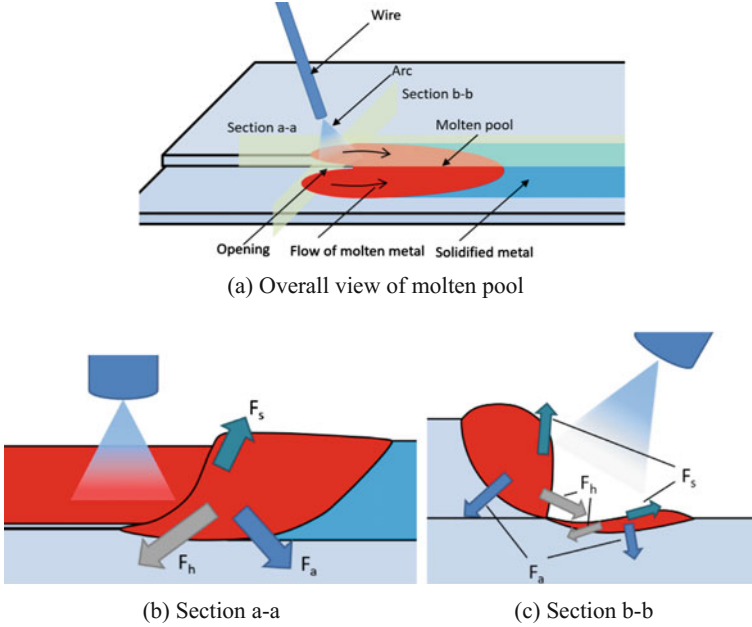


Fig. 7 Schematic diagram of molten pool

$$F_a = K \cdot I^2 \ln\left(\frac{R_2}{R_1}\right) \tag{5}$$

$$F_h = \rho' \cdot g \cdot h \tag{6}$$

where  $K$  is a coefficient;  $R_1$  is the radius of the arc at the welding electrode;  $R_2$  is the radius of the arc at the base plate;  $\rho'$  is the density of molten metal ( $\text{g}/\text{mm}^3$ );  $g$  is the gravitational acceleration ( $\text{mm}^2/\text{s}$ ); and  $h$  is the depth of molten metal (mm).

When  $F_a > F_h + F_s$ , the molten metal at the junction was pushed backwards and the molten metal at the foreparts was pushed outwards. The  $F_a$  is proportional to the second-order of current. That's why the opening size increased when the current increased. Considering the arc voltage, the influenced area by the arc was associated with the arc voltage. That means higher arc voltage causes more points exerted by arc force. This is considered to have caused the increase of integral arc force of every part and then expanded the opening. The travel speed affected the  $F_h$  due to the change of molten metal thickness. In this condition of high travel speed, the effect of  $F_a$  was also superior to the effect of  $F_h + F_s$  and same phenomenon happened.

On the contrary, at lower current, arc voltage or travel speed, the molten metal would shrink the opening. At lower current, the  $F_a$  became smaller accordingly. At lower arc voltage, the  $R_2$  shrank and the  $R_2/R_1$  decreased. Therefore, according to

the Eq. (5), the integral  $F_a$  reduced due to the reduction of influenced area by arc. The molten metal thickened at lower travel speed due to the increase of amount of molten metal. In these conditions, the  $F_a$  was inferior to the  $F_h + F_s$ . Therefore, the opening was not obvious.

Nevertheless, this doesn't mean the higher these parameters are, the better the weld beam is. As mentioned before, at the exorbitant arc voltage, the opening could be covered by molten metal and thus large blowholes existed in the weld beam. At the same time, the BCM humps could be caused in some parts of weld beam. The capillary instability humping model could be used to explain the BCM hump. When the length of liquid cylinder exceeds the critical length of instability, the liquid cylinder separates into a series of beads [19]. The upper forepart would act as a liquid cylinder. At exorbitant arc voltage, the liquid cylinder at upper edge might be too long due to long opening, and as a result, the BCM humps were formed. On the other hand, at excessive travel speed, the GRM humps could appeared in the weld beam. The GRM humps are related to the wall jet in high speed and current welding according to the research of Nguyen [20]. In the experiment at 1.6 m/min, the upper forepart and lower forepart of molten pool could be considered as two wall jets. When arc traveled rapidly, the rear of wall jet solidified firstly due to fast cooling and then the molten metal behind it formed the hump. Therefore, moderate voltage should be taken, and the travel speed should fit with the current and voltage.

Above all, the optimized parameters were selected. A sound weld beam was obtained with these parameters (Fig. 6c), and it was compared with a typical weld beam with other parameters (Fig. 8). The porosities reduced significantly with the optimized parameters. Although there were still several small blowholes in the optimized weld beam, the tensile strength of joint didn't decline.

Parameters	X-ray radiography
Optimized: $I_p=600A$ ; $U_m = 23V$ ; $v=1.35m/min$	
Other: $I_p=450A$ ; $U_m = 23V$ ; $v=1m/min$	

Fig. 8 Reduction of porosities in weld beam with optimized parameters

## 4 Conclusion

In present work, galvanized steel sheets in a zero-gap lap joint configuration were welded in pulse-MAG with different currents, arc voltages and travel speeds. During welding, the molten pool and metal transfer were observed through high-speed camera.

In the molten pool, there was an opening dividing the forepart into two parts. The size of opening increased with the increase of current. The current was a determined factor of arc force. And the peak current needed be high enough, because strong arc force was required to form the opening.

The arc voltage affected the stability of metal transfer and opening. At low voltage, the droplet couldn't detach, and spatters increased because of short-circuiting. At high arc voltage, the opening could be covered partially by the surging molten metal, and the BCM humps were formed. A moderate arc voltage was necessary to stably transfer metal from wire to molten pool.

The amount of metal per unit in molten pool changes at different travel speeds. The excessive molten metal obstructed the escape path of zinc vapor at low travel speed. At high speed, the humping phenomenon happened. The travel speed needs to fit with the current and voltage.

Optimized parameters were used to weld the galvanized steel sheets. The porosities in weld beam reduced significantly compared with other parameters. The porosity resistance could be improved by creating an appropriate stable opening with optimized parameters according to the welding condition.

## References

1. Yang S, Wang J, Carson BE et al (2013) Vacuum-assisted laser welding of zinc-coated steels in a gap-free lap joint configuration. *Weld J* 92(7):197s–204s
2. Yang SL, Kovacevic R (2009) Welding of galvanized dual-phase 980 steel in a gap-free lap joint configuration. *Weld J* 88:168–178
3. Jeric A, Grabec I, Govekar E (2009) Laser droplet welding of zinc coated steel sheets. *Sci Technol Weld Joining* 14(4):662–668
4. Pieters R, Richardson IM (2005) Laser welding of zinc coated steel in overlap configuration with zero gap. *Sci Technol Weld Joining* 10(2):142–144
5. Akhter R, Steen WM, Watkins KG (1991) Welding zinc-coated steel with a laser and the properties of the weldment. *J Laser Appl* 3(2):9–20
6. American Welding Society (1972) Welding zinc-coated steel. American Welding Society, Miami, pp 10–24
7. Pennington EJ (1987) Laser welding of galvanized steel. US Patent 4642446, 10 Feb 1987
8. Dasgupta A et al (2000) Alloying based laser welding of galvanized steel. In: Proceedings of international conference on applications of lasers and electro optics, Laser Institute of America, Dearborn, pp 38–45
9. Dasgupta A et al (2006) A novel method for lap welding of automotive sheet steel using high power CW CO<sub>2</sub> laser. Proceeding of the 4th international congress on laser advanced materials processing. ICLAMP, Kyoto, pp 1–5

10. Gualini M, Iqbal S, Grassi F (2006) Modified dual-beam method for welding galvanized steel sheets in lap configuration. *J Laser Appl* 18(3):185–191
11. Iqbal S, Gualini M, Rehman A (2010) Dual beam method for laser welding of galvanized steel: experimentation and prospects. *Opt Laser Technol* 42(1):93–98
12. Gu H, Mueller R (2001) Hybrid welding of galvanized steel sheet. In: 20th international congress on applications of lasers & electro-optics(ICALEO), Jacksonville, America, p 13–19
13. Matsui H, Suzuki H, Yamada M (1992) Reduction of blowholes in high-speed arc welding of ot-dip galvanised steel sheets. *Weld Int* 12(6):432–439
14. Schmidt M, Otto A, Kageler C (2008) Analysis of YAG laser lap-welding of zinc coated steel sheets. *CIRP Ann Manufact Technol* 57:213–216
15. Ahsan M, Kim YR, Kim CH et al (2016) Porosity formation mechanisms in cold metal transfer (CMT) gas metal arc welding (GMAW) of zinc coated steels. *Sci Technol Weld Joining* 21(3):209–215
16. Izutani S, Yamazaki K, Suzuki R (2013) New welding process, “J-Solution™ Zn”, suitable for galvanized steel in the automotive industry. *Kobelco Technol Rev* 32:16–23
17. Kodama S, Ishida Y, Furusako S et al (2013) Arc welding technology for automotive steel sheets. *Nippon Steel Tech Rep* 103:83–90
18. Kim YS, Eagar TW (1993) Analysis of metal transfer in gas metal arc welding. *Welding J* 1:269s–278s
19. Soderstrom E, Mendez P (2006) Humping mechanisms present in high speed welding. *Sci Technol Weld Joining* 11(5):572–579
20. Nguyen TC, Weckman DC, Johnson DA et al (2005) The humping phenomenon during high speed gas metal arc welding. *Sci Technol Weld Joining* 10(4):447–459